Published in final edited form as:
ACS Med Chem Lett. ; 3(5): 402–406. doi:10.1021/ml300038t.

HIV-1 Integrase Inhibitor-Inspired Antibacterials Targeting Isoprenoid Biosynthesis

Yonghui Zhang[#,†,‡,*], **Fu-Yang Lin**[‡,‡], **Kai Li**[†,‡], **Wei Zhu**[‡], **Yi-Liang Liu**[‡], **Rong Cao**[†], **Ran Pang**[Δ], **Eunhae Lee**[Δ], **Jordan Axelson**[†], **Mary Hensler**[§], **Ke Wang**[†], **Katie J. Molohon**[¥], **Yang Wang**[†], **Douglas A. Mitchell**[†,¥,¶], **Victor Nizet**[§], and **Eric Oldfield**[†,‡,*]

[#]PrenylX Research Institute, Zhangjiagang, 215600, P.R. China

[†]Department of Chemistry, University of Illinois at Urbana-Champaign, Urbana, IL, 61801, USA

[‡]Center for Biophysics & Computational Biology, University of Illinois at Urbana-Champaign, Urbana, IL, 61801, USA

[Δ]School of Molecular and Cellular Biology, University of Illinois at Urbana-Champaign, Urbana, IL, 61801, USA

[¥]Department of Microbiology, University of Illinois at Urbana-Champaign, Urbana, IL, 61801, USA

[¶]Institute for Genomic Biology, University of Illinois at Urbana-Champaign, Urbana, IL, 61801, USA

[§]Department of Pediatrics and Skaggs School of Pharmacy and Pharmaceutical Sciences, University of California, San Diego, La Jolla, CA, 92093, USA

Abstract

We report the discovery of antibacterial leads, keto- and diketo-acids, targeting two prenyl transferases: undecaprenyl diphosphate synthase (UPPS) and dehydrosqualene synthase (CrtM). The leads were suggested by the observation that keto- and diketo-acids bind to the active site Mg^{2+}/Asp domain in HIV-1 integrase, and similar domains are present in prenyl transferases. We report the x-ray crystallographic structures of one diketo-acid and one keto-acid bound to CrtM, which supports the Mg^{2+} binding hypothesis, together with the x-ray structure of one diketo-acid bound to UPPS. In all cases, the inhibitors bind to a farnesyl diphosphate substrate-binding site. Compound **45** had cell growth inhibition MIC_{90} values of ~250–500 ng/mL against *S. aureus*, 500 ng/mL against *Bacillus anthracis*, 4 μg/mL against *Listeria monocytogenes* and *Enterococcus faecium*, and 1 μg/mL against *Streptococcus pyogenes* M1, but very little activity against *E. coli* (DH5α, K12) or human cell lines.

Keywords

anti-bacterials; isoprenoid biosynthesis; HIV integrase; undecaprenyl diphosphate synthase; dehydrosqualene synthase

There is currently an urgent need for new types of anti-bacterials exhibiting novel modes of action, due to the rapid rise in drug resistance,[1] and isoprenoid biosynthesis[2] is one attractive

*Corresponding Author yhzhang30@yahoo.com. *eo@chad.scs.uiuc.edu.
‡These authors contributed equally.

Supporting Information. X-ray study, synthesis and characterization of the screening library compounds. This material is available free of charge via the Internet at http://pubs.acs.org.

target. For example, cell wall biosynthesis can be inhibited by targeting farnesyl diphosphate synthase (FPPS) or undecaprenyl diphosphate synthase (UPPS), involved in lipid I biosynthesis (Figure 1). In addition, in *S. aureus*, formation of the virulence factor staphyloxanthin[3] can be blocked by inhibiting dehydrosqualene synthase (CrtM), resulting in a lowering of the anti-oxidant shield to host derived ROS[4] (Figure 1). The bisphosphonate class of drugs such as zoledronate (**1**, Chart 1) are potent, low nM inhibitors of FPPS, but **1** has little antibacterial activity (due presumably to lack of cell penetration), although more lipophilic bisphosphonates such as **2** (BPH-210, Chart 1) have modest activity (IC_{50} ~30 μM) against *E. coli*.[5] More lipophilic bisphosphonates also potently target UPPS,[6] as well as CrtM[4], but again they have essentially no activity in bacteria. Replacing one phosphonate group by a sulfonate to form a phosphonosulfonate results, however, in potent CrtM inhibitors (e.g. **3**, BPH-652, Chart 1, IC_{50} ~ 7.9 μM, K_i ~ 80 nM) that also blocks carotenoid pigment formation in cells (IC_{50} ~110 nM).[7] In addition, there has recently been interest in developing phosphorus-free prenyl transferase inhibitors, which might have even more drug-like properties. For example, Jahnke et al. reported a series of FPPS inhibitors, dicarboxylic acids, that bound to a novel, allosteric site.[8] In addition, other species such as tetramic acid UPPS inhibitors have been described (e.g. **4,** Chart 1),[9] but to date their x-ray structures have not been reported, although an allosteric model has been proposed.[10]

A key component of the active site of most prenyl transferases is a Mg^{2+}/Asp motif that interacts with a substrate's diphosphate group. We reasoned that HIV-1 integrase (IN) inhibitors[11] might provide clues for new prenyl transferase inhibitors, since IN contains a similar Asp/Mg^{2+} motif[12] and IN inhibitors such as **5** (L-708,906, Chart 1)[13] and **6** (elvitegravir, Chart 1)[14], diketo-acids and keto-acids, respectively, are thought to bind at or near the Mg^{2+}/Asp motif in the IN active site.[15] In addition, many other IN inhibitors like raltegravir, dolutegravir, MK2048 etc (structures not shown) have been found to bind Mg^{2+}.[15b, 16]

We thus made a small screening library (38 compounds) of IN inhibitor-inspired molecules and their structures and inhibition of *S. aureus* CrtM, *E. coli* UPPS and *S. aureus* UPPS are shown in Figure S1. Most compounds were amide-diketo acids (**7**–**40**, class I, Figure S1) and were conveniently prepared from the synthon (*Z*)-2,2-dimethyl-5-carboxymethylene-1,3-dioxolan-4-one[17] by amine coupling. Among these compounds, **7** (Chart I) inhibited CrtM with IC_{50} ~24 μM, K_i ~ 250 nM (for comparison, K_i of **3** ~ 70 nM[7]), and blocked staphyloxanthin pigment formation (IC_{50} = 4 μM). Inhibitors of Class II were keto-acids, dihydropyridone-3-carboxylates, and were based on **6** (Elvitegravir) and dihydroquinoline-3-carboxylic acid IN inhibitors[18], which again are thought to bind *via* their carboxyl and carbonyl oxygens to Mg^{2+}/Asp.[19] We made two analogs, **41**, **42** (Chart I), with alkoxy-aryl tails to mimic the substrate FPP. The longer-chain species **42** had no activity, but the shorter chain species **41** had a CrtM IC_{50}= 45 μM, K_i = 450 nM and a loss of pigmentation IC_{50} of 33 μM.

To see how these inhibitors bound to CrtM, we carried out co-crystallization and soaking experiments with **7** (Class I) and **41** (Class II) and obtained crystals (by soaking) that diffracted to 2.3 Å and 1.9Å, respectively. Full x-ray crystallographic data and structure refinement details are given in Supporting Information, Table S1. Electron density results for **7** are shown in Figure 2a and indicate the presence of **7** in addition to one molecule of farnesyl monophosphate (FMP) that co-purified with the protein. The identity of FMP was further confirmed by LC-MS (Supporting Information, Figure S2) and the electron density results (Figure 2a). The diphenyl ether fragment in **7** (cyan) binds into the CrtM S1 site[20], and is shown in Figure 2b superimposed on one of the *S-thiolo*-farnesyl diphosphate (FSPP) inhibitors (in yellow, green) whose structures were reported previously.[4] This binding mode is similar to that seen with the phosphonosulfonate **3** (Figure 2c), with the diketo-acid head-group interacting with two of the three Mg^{2+} ($Mg^{2+}_{B,C}$) seen in the CrtM-FSPP structure (Figure 2d). The farnesyl side-chain in FMP bound to the S2 site and had a 0.8 Å rmsd from the S2 FSPP reported previously.[4] With **41**, the ligand electron density is again well defined (Figure 3a), and the crystallographic results show the side-chain binds in S2, similar to the farnesyl side-chain in the FSPP structures (Figure 3b), as well as the phosphonoacetamide analog of **7** (**43**, BPH-830[21], Figure 3c). There are 3 Mg^{2+} in the x-ray structure. However, these are not the Mg^{2+}_{ABC} seen in most prenyl transferases[22] but rather, Mg^{2+}_{BCD}. That is, there is a new Mg^{2+} binding site, Mg^{2+}_{D}. The dihydropyridone side-chain interacts with Mg^{2+}_{CD} but surprisingly, via the two ring oxygens, not the carboxylate (Figure 3d), which interacts with two water molecules (Supporting Information, Figure S3). These inhibition and structural results for **7** and **41** clearly support the Mg^{2+} binding hypothesis, at least for CrtM.

CrtM is a so-called head-to-head prenyl transferase so we next sought to see if any of the molecules synthesized might also inhibit the head-to-tail prenyl transferase FPPS, or the *cis*-prenyl transferase, UPPS. There was no activity against FPPS (probably due to the lack of a positively charged feature that mimics the carbocation involved in FPP biosynthesis) but most of the amide-diketo acids (Class I) were potent UPPS inhibitors with the most active one (**8**) having an IC_{50} ~ 240 nM and K_i ~ 120 nM, comparable to the most active bisphosphonate UPPS inhibitor BPH-629 (IC_{50} ~ 300 nM for *E. coli* UPPS)[6]. There are four different ligand-binding sites in UPPS (designated 1–4 in Ref 6) found with bisphosphonate inhibitors. This is not unexpected since the UPPS product, undecaprenyl diphosphate (UPP) contains 55-carbon atoms and is thus much larger than the (C_{15}) FPP substrate. In principle, then, novel inhibitors might occupy multiple binding sites.

Co-crystallization of *E. coli* UPPS with **9** (IC_{50} = 560 nM) produced well-formed crystals with *E. coli* UPPS, and the electron density was well resolved (Figure 4a). As can be seen in Figure 4b, **9** binds to site 1[6], the FPP binding site and, as can be seen in Figure 4c, **9** (in cyan) closely maps the FPP backbone structure (in yellow) with the diketo-acid fragment being located close to two of the three most essential residues in UPPS, D26 and N28 (Figure 4d). We found no evidence for the presence of Mg^{2+}, but this observation is not entirely unexpected since even with the 5 *E. coli* UPPS x-ray structures with strong Mg^{2+} chelators – bisphosphonates (PDB ID codes 2E98, 2E99, 2E9A, 2E9C, 2E9D),[6] Mg^{2+} was not observed.

The amide-diketo acids were not growth suppressive towards *S. aureus* or *E. coli*, perhaps due to the instability of the amide bond inside the cells, or a lack of cell permeability. However, **44** and **45** (aryldiketo acids, Class III), had good activity against *S. aureus* UPPS (**44**, IC_{50} = 0.73 μM, K_i = 230 nM; **45**, IC_{50} = 2.0 μM, K_i = 670 nM) and both were active against the USA300 (MRSA) strain of *S. aureus* with MIC_{90} values of 500 ng/mL (**44**) and 250–500 ng/mL (**45**). There was no appreciable activity against the Gram-negative *E. coli*, however, there was promising activity against other Gram-positives: ~ 500 ng/mL against *Bacillus anthracis* str. Sterne, ~ 4 μg/mL against *Listeria monocytogenes* and *Enterococcus faecium* U503, and ~ 1 μg/mL for *Streptococcus pyogenes* M1. While the precise mechanism of action of these compounds in each cell remains to be determined, UPPS inhibition is a likely candidate. In addition, we found low toxicity against a human cell line (MCF-7; IC_{50} ~30 μM), consistent with poor FPPS inhibition.

These results are important for several reasons. First, we tested the hypothesis that keto- and diketo-acids might inhibit prenyl transferase enzymes, based on the presence of Mg^{2+}/Asp motifs in their active sites – an "integrase inhibitor-inspired" approach. The best CrtM inhibitors had K_i ~ 250 nM and were active in blocking staphyloxanthin biosynthesis in *S. aureus*, and we solved two structures of lead compounds bound to CrtM. In both, the inhibitor head-groups bound to Mg^{2+}, while the side-chains bound to one or the other of the two FPP side-chain binding sites. Second, we tested this small library for FPPS and UPPS inhibition. There was no FPPS inhibition, but the most potent UPPS inhibitor had an IC_{50} = 240 nM, and we determined the structure of one such lead bound to *E. coli* UPPS – the first UPPS x-ray structure reported for a non-bisphosphonate inhibitor. We also found low toxicity and promising activity against a subset of Gram-positive bacteria with MIC_{90} values as low as 250–500 ng/mL against USA300 *S. aureus* and 500 ng/mL against *Bacillus anthracis* str. Sterne, and low activity against *E. coli* and a human cell line. Overall, these results indicate that integrase-inspired inhibitors may be engineered into drug leads that target isoprenoid biosynthesis.

Supplementary Material

Refer to Web version on PubMed Central for supplementary material.

Acknowledgments

This work was supported by the United States Public Health Service (NIH grant 5R01AI074233-16 to EO) and the NIH Director's New Innovator Award Program (DP2 OD008463 to DAM). KJM was supported in part by a NIH Cellular and Molecular Biology Training Grant (T32 GM007283). The Advanced Photon Source was supported by Department of Energy Contract DE-AC02-06CH11357. The Life Science Collaborative Access Team Sector 21 was supported by the Michigan Economic Development Corporation and Michigan Technology Tri-Corridor (Grant 085P000817). We thank Andrew H.-J. Wang of Institute of Biological Chemistry, Academia Sinica (Taipei, Taiwan) for providing *E. coli* UPPS plasmids and *S. aureus* CrtM plasmids.

ABBREVIATIONS

CrtM	dehydrosqualene synthase
UPPS	undecaprenyl diphosphate synthase
FPPS	farnesyl diphosphate synthase
FPP	farnesyl diphosphate
(FMP)	farnesyl monophosphate
FSPP	*S-thiolo*-farnesyl diphosphate
IN	HIV-integrase

REFERENCES

1. Walsh CT, Fischbach MA. Repurposing libraries of eukaryotic protein kinase inhibitors for antibiotic discovery. Proc. Natl. Acad. Sci. U. S. A. 2009; 106:1689–1690. [PubMed: 19193851]
2. (a) Oldfield E. Targeting isoprenoid biosynthe/is for drug discovery: bench to bedside. Acc. Chem. Res. 2010; 43:1216–1226. [PubMed: 20560544] (b) Oldfield E, Lin FY. Terpene biosynthesis: modularity rules. Angew. Chem. Int. Ed. Engl. 2012; 51:1124–1137. [PubMed: 22105807]
3. Liu GY, Essex A, Buchanan JT, Datta V, Hoffman HM, Bastian JF, Fierer J, Nizet V. *Staphylococcus aureus* golden pigment impairs neutrophil killing and promotes virulence through its antioxidant activity. J. Exp. Med. 2005; 202:209–215. [PubMed: 16009720]
4. Liu CI, Liu GY, Song Y, Yin F, Hensler ME, Jeng WY, Nizet V, Wang AH, Oldfield E. A cholesterol biosynthesis inhibitor blocks *Staphylococcus aureus* virulence. Science. 2008; 319:1391–1394. [PubMed: 18276850]
5. Leon A, Liu L, Yang Y, Hudock MP, Hall P, Yin F, Studer D, Puan KJ, Morita CT, Oldfield E. Isoprenoid biosynthesis as a drug target: bisphosphonate inhibition of *Escherichia coli* K12 growth and synergistic effects of fosmidomycin. J. Med. Chem. 2006; 49:7331–7341. [PubMed: 17149863]

6. Guo RT, Cao R, Liang PH, Ko TP, Chang TH, Hudock MP, Jeng WY, Chen CK, Zhang Y, Song Y, Kuo CJ, Yin F, Oldfield E, Wang AH. Bisphosphonates target multiple sites in both *cis*- and *trans*-prenyltransferases. Proc. Natl. Acad. Sci. U. S. A. 2007; 104:10022–10027. [PubMed: 17535895]
7. Song Y, Lin FY, Yin F, Hensler M, Rodrigues Poveda CA, Mukkamala D, Cao R, Wang H, Morita CT, Gonzalez Pacanowska D, Nizet V, Oldfield E. Phosphonosulfonates are potent, selective inhibitors of dehydrosqualene synthase and staphyloxanthin biosynthesis in *Staphylococcus aureus*. J. Med. Chem. 2009; 52:976–988. [PubMed: 19191557]
8. Jahnke W, Rondeau JM, Cotesta S, Marzinzik A, Pelle X, Geiser M, Strauss A, Gotte M, Bitsch F, Hemmig R, Henry C, Lehmann S, Glickman JF, Roddy TP, Stout SJ, Green JR. Allosteric non-bisphosphonate FPPS inhibitors identified by fragment-based discovery. Nat. Chem. Biol. 2010; 6:660–666. [PubMed: 20711197]
9. Peukert S, Sun Y, Zhang R, Hurley B, Sabio M, Shen X, Gray C, Dzink-Fox J, Tao J, Cebula R, Wattanasin S. Design and structure-activity relationships of potent and selective inhibitors of undecaprenyl pyrophosphate synthase (UPPS): tetramic, tetronic acids and dihydropyridin-2-ones. Bioorg. Med. Chem. Lett. 2008; 18:1840–1884. [PubMed: 18295483]
10. Lee LV, Granda B, Dean K, Tao J, Liu E, Zhang R, Peukert S, Wattanasin S, Xie X, Ryder NS, Tommasi R, Deng G. Biophysical investigation of the mode of inhibition of tetramic acids, the allosteric inhibitors of undecaprenyl pyrophosphate synthase. Biochemistry. 2010; 49:5366–5376. [PubMed: 20476728]
11. HIV-1 Integrase: Mechanism and Inhibitor Design. 2011Neamati, N. John Willey & Sons Inc.Hoboken, New Jersey
12. Goldgur Y, Dyda F, Hickman AB, Jenkins TM, Craigie R, Davies DR. Three new structures of the core domain of HIV-1 integrase: an active site that binds magnesium. Proc. Natl. Acad. Sci. U. S. A. 1998; 95:9150–9154. [PubMed: 9689049]
13. Hazuda DJ, Felock P, Witmer M, Wolfe A, Stillmock K, Grobler JA, Espeseth A, Gabryelski L, Schleif W, Blau C, Miller MD. Inhibitors of strand transfer that prevent integration and inhibit HIV-1 replication in cells. Science. 2000; 287:646–650. [PubMed: 10649997]
14. Sato M, Kawakami H, Motomura T, Aramaki H, Matsuda T, Yamashita M, Ito Y, Matsuzaki Y, Yamataka K, Ikeda S, Shinkai H. Quinolone carboxylic acids as a novel monoketo acid class of human immunodeficiency virus type 1 integrase inhibitors. J. Med. Chem. 2009; 52:4869–4882. [PubMed: 19719237]
15. (a) Grobler JA, Stillmock K, Hu B, Witmer M, Felock P, Espeseth AS, Wolfe A, Egbertson M, Bourgeois M, Melamed J, Wai JS, Young S, Vacca J, Hazuda DJ. Diketo acid inhibitor mechanism and HIV-1 integrase: implications for metal binding in the active site of phosphotransferase enzymes. Proc. Natl. Acad. Sci. U. S. A. 2002; 99:6661–6666. [PubMed: 11997448] (b) Hare S, Gupta SS, Valkov E, Engelman A, Cherepanov P. Retroviral intasome assembly and inhibition of DNA strand transfer. Nature. 2010; 464:232–236. [PubMed: 20118915]
16. (a) Hare S, Smith SJ, Métifiot M, Jaxa-Chamiec A, Pommier Y, Hughes S, Cherepanov P. Structural and functional analyses of the second-generation integrase strand transfer inhibitor dolutegravir (S/GSK 1349572). Mol. Pharmacol. 2011; 80:565–572. [PubMed: 21719464] (b) Hare S, Vos AM, Clayton RF, Thuring JW, Cummings MD, Cherepanov P. Molecular mechanisms of retroviral integrase inhibition and the evolution of viral resistance. Proc. Natl. Acad. Sci. U. S. A. 2010; 107:20057–20062. [PubMed: 21030679]
17. Zhu K, Simpson JH, Delaney EJ, Nugent WA. Synthesis of *Z*-5-carboxymethylene-1,3-dioxolan-4-ones: a better way. J.Org. Chem. 2007; 72:3949–3951. [PubMed: 17432907]
18. Sechi M, Rizzi G, Bacchi A, Carcelli M, Rogolino D, Pala N, Sanchez TW, Taheri L, Dayam R, Neamati N. Design and synthesis of novel dihydroquinoline-3-carboxylic acids as HIV-1 integrase inhibitors. Bioorg. Med. Chem. 2009; 17:2925–2935. [PubMed: 19026554]
19. Vandurm P, Cauvin C, Guiguen A, Georges B, Le Van K, Martinelli V, Cardona C, Mbemba G, Mouscadet JF, Hevesi L, Van Lint C, Wouters J. Structural and theoretical studies of [6-bromo-1-(4-fluorophenylmethyl)-4(1H)-quinolinon-3-yl)]-4-hydroxy-2-oxo- 3-butenoic acid as HIV-1 integrase inhibitor. Bioorg. Med. Chem. Lett. 2009; 19:4806–4809. [PubMed: 19556126]
20. Lin FY, Liu CI, Liu YL, Zhang Y, Wang K, Jeng WY, Ko TP, Cao R, Wang AH, Oldfield E. Mechanism of action and inhibition of dehydrosqualene synthase. Proc. Natl. Acad. Sci. U. S. A. 2010; 107:21337–21342. [PubMed: 21098670]

21. Song Y, Liu CI, Lin FY, No JH, Hensler M, Liu YL, Jeng WY, Low J, Liu GY, Nizet V, Wang AH, Oldfield E. Inhibition of staphyloxanthin virulence factor biosynthesis in *Staphylococcus aureus*: in vitro, in vivo, and crystallographic results. J. Med. Chem. 2009; 52:3869–3880. [PubMed: 19456099]

22. Aaron JA, Christianson DW. Trinuclear Metal Clusters in Catalysis by Terpenoid Synthases. Pure Appl. Chem. 2010; 82:1585–1597. [PubMed: 21562622]

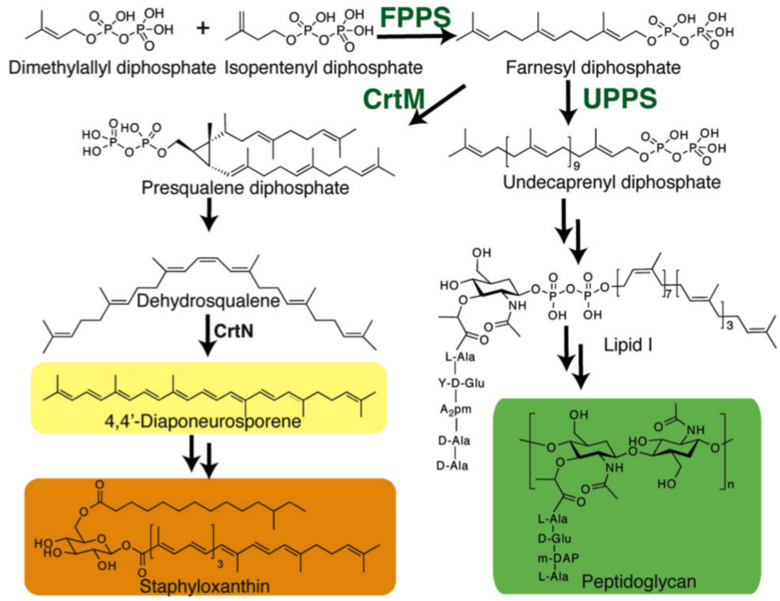

Figure 1.

Biosynthetic reactions catalyzed by CrtM and UPPS, with the end products of the pathways shown.

NIH-PA Author Manuscript
NIH-PA Author Manuscript

NIH-PA Author Manuscript

NIH-PA Author Manuscript

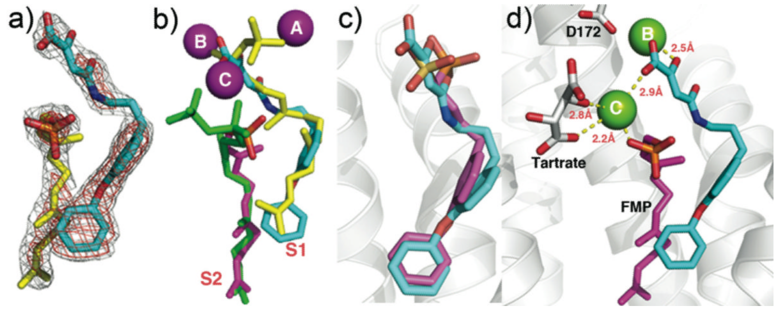

Figure 2.

CrtM crystallographic structures. a) **7** (cyan) plus FMP (yellow) electron density, bound to CrtM. b) **7** (cyan) bound to CrtM, superimposed on two FSPP molecules (yellow, green; PDB ID code 2ZCP). Also shown is the farnesyl monophosphate (magenta) that co-crystallized. The Mg^{2+} are from the FSPP structure. c) Comparison between **7** (cyan) and **3** (magenta, PDB ID code 2ZCQ) bound to CrtM. Both diphenyl ether side-chains bind in S1. d) Interactions between **7** (cyan), FMP (magenta) and Mg^{2+} in CrtM.

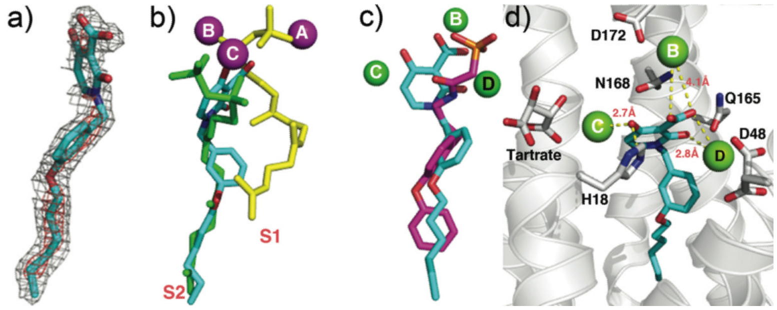

Figure 3.

CrtM crystallographic structures. a) Electron density of **41** bound to CrtM. b) Structure of **41** (cyan) bound to CrtM shown superimposed on two FSPP molecules (yellow, green). c) Comparison between **41** (cyan) and the phosphonoacetamide analog of **7**(compound 43, BPH-830)[21] (magenta) bound to CrtM (PDB ID code 2ZY1). d) Interactions between **41** (cyan) and Mg^{2+} in CrtM.

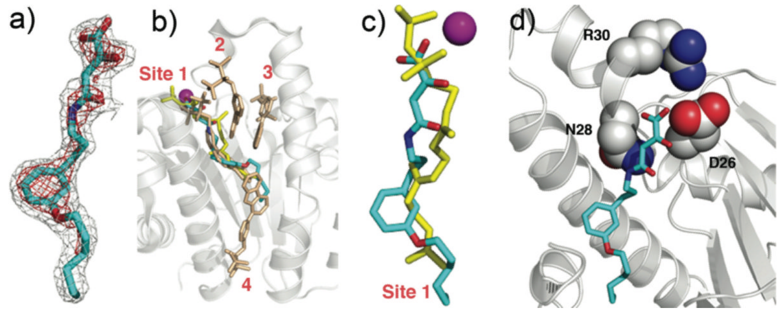

Figure 4.

UPPS crystallographic structures. a) Electron density of **9** bound to UPPS. b) Structure of **9** (cyan) bound to UPPS, superimposed on FSPP/Mg^{2+} (from PDB ID code 1X06) and 4 bisphosphonate inhibitors (PDB ID code 2E98). c) Superposition of **9** (cyan) on FSPP (yellow) in site-1 in UPPS. The Mg^{2+} is from the FSPP structure. d) The diketo-acid head-group of **9** binds into the active site of UPPS and interacts with D26 and N28.

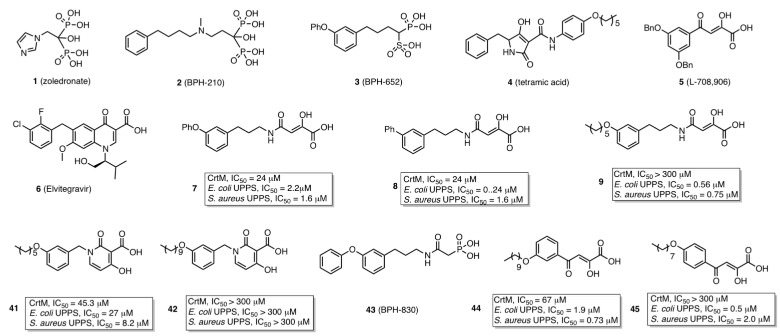

Chart 1.

Chemical structures of selected compounds and the inhibition of CrtM, *E. coli* UPPS and *S. aureus* UPPS by 7, 8, 9, 41, 42, 44, 45.